Catalysis Today 169 (2011) 24–28

Contents lists available at ScienceDirect

Catalysis Today

journal homepage: www.elsevier.com/locate/cattod

Cluster–support interaction in Au–Fe_3O_4 system

N. Spiridis[a,*], R.P. Socha[a], B. Handke[b,1], J. Haber[b], M. Szczepanik[b], J. Korecki[a,b]

[a] Institute of Catalysis and Surface Chemistry, Polish Academy of Sciences, Niezapominajek 8, 30-239 Kraków, Poland
[b] Faculty of Physics and Applied Computer Science, AGH University of Science and Technology, 30-059 Kraków, Poland

ARTICLE INFO

Article history:
Available online 22 October 2010

Keywords:
Cluster–support interaction
Gold
$Fe_3O_4(0\,0\,1)$
STM
XPS
Mössbauer spectroscopy

ABSTRACT

Cluster–support interaction in a Au–$Fe_3O_4(0\,0\,1)$ system was studied using scanning tunneling microscopy, X-ray photoemission spectroscopy and Mössbauer spectroscopy, in situ, under ultra high vacuum conditions. Deposition of 0.02–5 monolayers of Au resulted in the growth of two- and three-dimensional gold nano-cluster. The positive shift of the Au $4f_{7/2}$ electron binding energy for the smallest clusters was correlated with modification of the electronic structure in the surface magnetite layer, as found from Mössbauer analysis, leading to conclusion that a positive charging of small Au clusters can be responsible for their outstanding catalytic activity.

1. Introduction

Metal nanoclusters grown on single-crystalline oxide supports play an important role in model catalyst studies [1]. In such analyses of catalytic properties, modification of the cluster's electronic structure due to size effects is usually treated as the dominant factor. While the important role of the support in determination of the cluster morphology is indisputable [2,3], much less is known about the microscopic character of the cluster–support interaction and its influence on the oxide electronic properties.

The aim of this work was to study the modification of the electronic properties of a metal clusters/oxide support system. To this end, the formation and role of the metal/metal oxide interface has been studied for Au clusters deposited on the (0 0 1) surface of Fe_3O_4 epitaxial films grown on MgO(0 0 1). Gold supported on transition metal oxides is active in the oxidation of CO at low temperatures [4]. The catalytic activity strongly depends on the size of the Au nanoclusters, on their interaction with the oxide support and on their oxidation and charge state. A precondition for understanding catalytic processes on the atomic scale is the knowledge of the atomic level structure and interactions at the cluster–support interface, which can be acquired by applying surface-science approaches to chosen model single-crystalline catalysts. Magnetite surfaces are especially attractive model oxide supports due to their native conductivity, which facilitates imaging and spectroscopic studies. Recently, the electronic properties and chemical reactivity of gold nanoparticles and adatoms were studied on the (1 1 1) surface of single-crystal magnetite [5]. Here we use as the support magnetite $Fe_3O_4(0\,0\,1)$ films grown on MgO(0 0 1), and we present combined scanning tunneling microscopy (STM) and X-ray photoemission and conversion Mössbauer electron spectroscopy studies that have revealed strong electronic interaction between the gold cluster and the magnetite support.

2. Experimental methods

All experiments were done in situ under ultra high vacuum (UHV) in a system described previously [6]. Samples were obtained on single-crystalline MgO(0 0 1) substrates cleaved prior to their introduction into the UHV system (base pressure below 1×10^{-10} mbar). $Fe_3O_4(0\,0\,1)$ films with thickness between 20 and 40 nm were grown by Fe-vapor deposition in the presence of oxygen at the rate of about 1 nm/min, on substrate held at 250 °C. The growth of the magnetite films, controlled using the quartz crystal balance, was monitored by low-energy electron diffraction (LEED) and Auger electron spectroscopy (AES). STM images were acquired using an Aris1100 (Burleigh) STM head and electrochemically etched W-tips. Mössbauer spectra were measured by detection of the conversion and Auger electrons following the recoilless nuclear absorption (so called conversion-electron Mössbauer spectroscopy – CEMS). A small active area ^{57}Co γ-source was placed outside the UHV system, inside a stainless steel tube entering the chamber and illuminating the sample via a beryllium window. A large-opening channeltron (25 mm in diameter), placed a few millimeters from the sample, was used as the electron detector. The surface selectivity of the CEMS measurements

* Corresponding author.
E-mail address: ncspirid@cyf-kr.edu.pl (N. Spiridis).
[1] Present address: Faculty of Materials Science and Ceramics, AGH University of Science and Technology, 30-059 Kraków, Poland.

0920-5861/$ – see front matter © 2010 Elsevier B.V. All rights reserved.
doi:10.1016/j.cattod.2010.08.027

was enhanced using an ultrathin $^{57}Fe_3O_4$ surface probe layer on top of a $^{56}Fe_3O_4$ film. During deposition of the ^{57}Fe probe layer the sample temperature was decreased to 150 °C to avoid $^{56}Fe/^{57}Fe$ intermixing. Gold was deposited on the magnetite surface from a thermal source in doses ranging from a fraction of a monolayer (ML) to several MLs, where 1 ML of Au is taken as corresponding to 1.39×10^{15} atoms/cm^2 (atom density on the dense-packed Au(1 1 1) surface). The XPS measurements were made in situ using an R4000 Gammadata Scienta hemispherical analyzer and an Al Kα excitation source. The Fermi edge was used for calibration of the electron binding energy (BE) scale.

3. Results

3.1. Structure of the Fe_3O_4(0 0 1) surface

Magnetite crystallizes in the cubic inverse spinel structure with the lattice constant 0.843 nm. The oxygen ions form a close-packed cubic structure with Fe ions localized in two different interstitial sites, octahedral and tetrahedral. The 64 tetrahedral sites (A) in the unit cell are occupied by 8 trivalent Fe ions. Sixteen tri- and di-valent Fe ions occupying 32 octahedral sites (B) are randomly arranged at room temperature because of electron hopping, which averages the valence of the octahedral cations to $Fe^{2.5+}$. Surface termination and reconstruction of magnetite is a controversial problem [7]. The surface structure of (0 0 1)-oriented magnetite is usually discussed considering the bulk unit cell as composed of eight atomic sub-layers, which contain either only tetrahedral iron atoms in A sites (called A-layer) or oxygen and octahedral B iron ions (called B-layer). The B-layers contain twice as many iron atoms as the A-layers. The distance between A–A or B–B layers is about 0.21 nm, whereas the smallest interlayer (A–B) spacing is about 0.11 nm. None of the bulk terminated Fe_3O_4(0 0 1) surfaces (neither A nor B) are charge compensated, and the charge neutrality condition of the polar Fe_3O_4(0 0 1) is described as the driving force of the reconstruction. The reconstruction, intensively studied with different methods for single crystals [8,9] as well as for epitaxial films [10–15], is very sensitive to the preparation conditions. Different authors explain the reconstruction by oxygen vacancies [14], electronic effects [16] or Jahn–Teller distortion [17]. Recently, we showed that (0 0 1) termination can be controlled by a special preparation procedure [18]. Films prepared directly on MgO(0 0 1), as used in the present study, are terminated with an oxygen-rich layer (the B-layer) composed of oxygen and iron ions in the octahedral sub-lattice. The surface is characterized by the $\left(\sqrt{2} \times \sqrt{2}\right)$ R45° reconstruction, as seen in LEED patterns shown in Fig. 1a. The STM measurements presented in Fig. 1b and c clearly revealed details responsible for the reconstruction. In the larger 100 nm × 100 nm scan (Fig. 1b), irregular terraces are seen with an average step height of about 0.2 nm, which corresponds to the A–A or B–B layer spacing. Higher magnification (Fig. 1c) shows that the terraces are dominated by atomic rows, spaced by 0.6 nm, which are mutually perpendicular on neighboring terraces. Occasionally, there are also areas where the row orientation changes within a terrace. Additionally, a strong modulation of the intensity along the rows appears in some areas, forming the structure of dark "holes" responsible for the $\left(\sqrt{2} \times \sqrt{2}\right)$ R45° reconstruction. According to the surface symmetry, the rows are commonly interpreted as coming from Fe ions in octahedral sites. Thus, we conclude that the films are terminated with the B-layer. In our interpretation, the modulation along octahedral Fe rows, which is strongly bias-voltage dependent, comes from an electronic effect (e.g., charge ordering) rather than from oxygen vacancies [18].

3.2. Gold adsorption on the Fe_3O_4(0 0 1) surface – STM results

On B-layer-terminated Fe_3O_4(0 0 1) with the $\left(\sqrt{2} \times \sqrt{2}\right)$ R45° reconstruction, initial adsorption of gold at room temperature proceeds via cluster formation. Using STM, Jordan et al. [19] observed on a single crystal surface monoatomic-height Au clusters, typically 0.9 nm in diameter.

Our studies produced a somewhat different result. Room-temperature deposition of Au in the submonolayer coverage range (0.02–0.15 ML) resulted in the nucleation of small two- and three-dimensional clusters, as shown in Fig. 2a. The apparent cluster dimensions ranged from 0.8 nm to 2 nm in diameter and 0.2 nm to 0.7 nm in height. Most of the clusters were found on the terraces; however, there was a limited tendency toward nucleation at the step edges. Taking into account the high defect density on our Fe_3O_4(0 0 1) surface, heterogeneous nucleation at the defect sites on the terraces cannot be excluded. The nucleation phase was completed at a coverage below 0.3 ML, and the cluster then grew three-dimensionally with a maximum cluster density of about 10^{13}/cm^2. The clusters did not coalesce for the largest observed coverage of 5 ML, forming an assembly of separated islands, with average lateral dimensions of 7 nm and average height of 3 nm, as shown in Fig. 2b.

3.3. Spectroscopic data

XPS measurements were performed on the clean Fe_3O_4(0 0 1) surface and on the gold adsorbate in the coverage range of 0.02–5 ML. The clean surface shows stoichiometric composition of Fe_3O_4 with an Fe/O ratio equal to 0.751. For the smallest Au coverage of 0.02 ML, the electron binding energy of Au $4f_{7/2}$ core excitation was 84.4 eV. With increasing Au coverage, as shown in

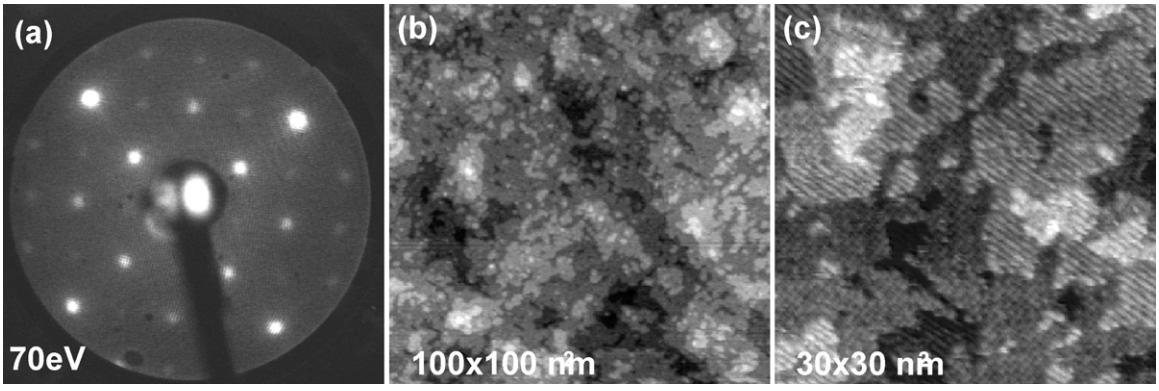

Fig. 1. LEED pattern (a) and STM images ((b) and (c)) for the surface of a Fe_3O_4(0 0 1) film deposited at 250 °C. STM images are taken at the sample bias voltage $V_s = +0.9 \pm 0.1$ V and tunnelling current about 1 nA.

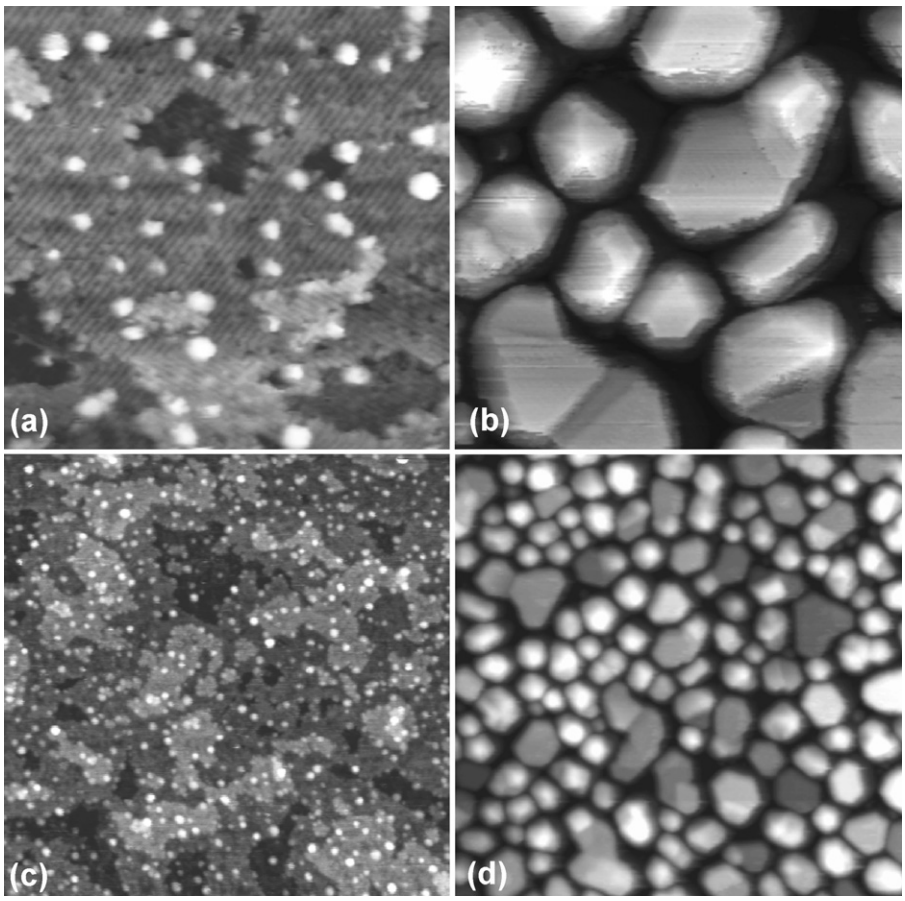

Fig. 2. STM images of a Fe_3O_4(0 0 1) surface with Au adsorbate (room temperature deposition): 0.03 ML ((a) and (c)), 5 ML ((b) and (d)). The scan size is 30 nm × 30 nm and 100 nm× 100 nm for ((a), (b)) and ((c), (d)), respectively.

Fig. 3, the maximum of Au $4f_{7/2}$ excitation decreased, reaching the Au bulk value of 84.0 eV for the large three-dimensional clusters observed for the 5-ML coverage. The positive shift of the binding energy for small metal clusters, called the final-state effect, is interpreted as temporal charging of the nanoparticle due to the photoionization process [20,21]. This shift, which scales with the reciprocal of particle diameter, can be as large as 1 eV for 1-nm gold nanoparticles [22]. In this context, the shift of 0.4 eV found in this study for clusters with an average diameter of 1 nm indicates that an opposite effect, the ground-state effect, may be overlapping with the final-state effect. The ground-state effect for Au-clusters should be similar to that for the Au-surface, for which the surface-atom 4f shifts are negative and close to 0.4 eV [23]. Furthermore, the gold clusters can be charged due to the electron transfer to the support, and this effect is supposed to be crucial for the catalytic activity [5]. Because the separation of these effects is difficult [24], verification of the charge state of our gold nanoparticles based only on the XPS data is practically impossible.

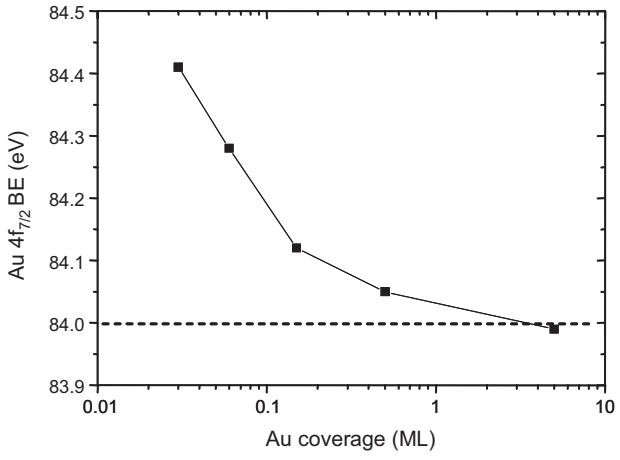

Fig. 3. Au 4f binding energy plotted as a function of the Au coverage on the Fe_3O_4(0 0 1) surface. Dashed line shows BE for a bulk Au surface [23].

Additional information concerning the charge transfer came from CEMS measurements. Modifications in the electronic structure of the Fe_3O_4(0 0 1) surface under the influence of gold adsorption were directly seen by Mössbauer spectroscopy using an 8-Å $^{57}Fe_3O_4$ probe layer deposited on top of a $^{56}Fe_3O_4$ epitaxial film. Mössbauer spectroscopy has numerous advantages when applied to thin magnetite films. The method is crystal-site and valence-state sensitive, and by using ^{57}Fe probes [6], its spatial resolution can be enhanced into the monolayer range. Detailed CEMS studies of the Fe_3O_4(0 0 1) surface were published earlier [6]. The most important finding concerned strong modifications of the surface electronic properties that were distinctly reflected in the spectra. The Mössbauer spectrum of bulk-like magnetite at room temperature, when the electron hopping process is fast, is characterized by two sextets. The one with the hyperfine magnetic field B_{hf} = 48.8 T and the isomer shift IS = 0.27 mm/s relative to α-Fe corresponds to the Fe_A^{3+} ions at the tetrahedral A-sites. The second one, with B_{hf} = 45.7(2) T and IS = 0.65 mm/s, is the $Fe_B^{2.5+}$-like average signal from the cations at the octahedral B sites. Fe_B^{+2} and Fe_B^{3+} are indistinguishable due to fast electron transfer (electron hopping), which is faster ($\tau \sim 1$ ns) than the ^{57}Fe excited state lifetime (98 ns). The intensity ratio $\beta = I(B)/I(A)$ of the two spectral

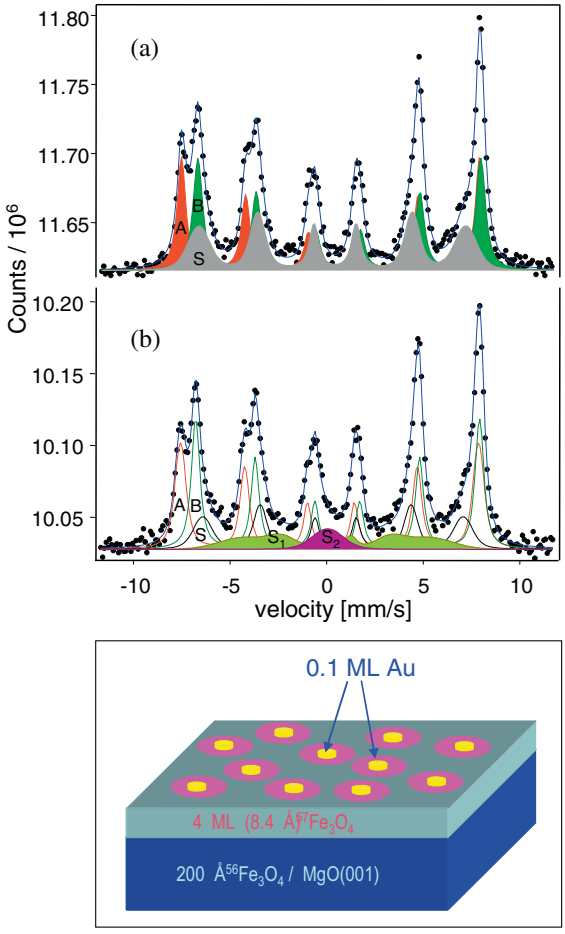

Fig. 4. CEMS spectra for a clean $Fe_3O_4(0\,0\,1)$ surface with a 8 Å $^{57}Fe_3O_4(0\,0\,1)$ Mössbauer probe layer (a) and after deposition of 0.1 ML of Au (b). The cartoon illustrates the surface extent of the influence of the gold clusters on the electronic structure of the oxide support deducted from the measurements.

components is a sensitive measure of the stoichiometry. Assuming that the room-temperature ratio of the recoil-free fractions f_B/f_A for the B and A sites is 0.94 [7], the intensity ratio β for perfect stoichiometry should be 1.88. For the CEMS spectrum of the magnetite surface, shown in Fig. 4a, these two components, (A) – tetrahedral and (B) – octahedral, are accompanied by a broad-line sextet (S), which we interpret as coming from the outermost atomic layer of magnetite. The 0.8-nm $^{57}Fe_3O_4$ probe layer nominally contains close to four atomic layers. Within our interpretation, these four atomic layers are composed of the following: two of tetrahedral A-type, contributing to component (A), one of octahedral B-type, contributing to component (B) and one surface octahedral contributing to component (S). The experimentally observed intensity ratio of the spectral components (A):(B):(S) is 1:1.06:0.98, in perfect agreement with nominal iron occupation of the tetrahedral and octahedral layers. The hyperfine parameters of the surface octahedral component (S) are distinctly different from the bulk values. The broken translational symmetry is reflected in the reduction of the B_{hf} value [42.87 T, compared to 45.42 T for component (B)], while a certain degree of surface disorder, as seen in STM images, results in a considerable distribution of B_{hf} [$\Delta B_{hf}/B_{hf}$ = 6.6%, compared to 1% for component (B)]. The valence state of the surface iron ions can be determined from the isomer shift, which is reduced from 0.67 mm/s for component (B) to 0.41 for component (S). The isomer shift depends on the electron density at the nucleus, $|\Psi(0)|^2$. Only s-electrons contribute to $|\Psi(0)|^2$, and the Fe(II) and Fe(III) ions have the same number of s-electrons. However, they differ in the number of d-electrons, which induces a difference in 3s-electron density at the nuclei of Fe(II) and Fe(III). These electrons have a high probability of being further away from the nucleus than the 3d-electrons. The Coulomb interaction between the 3d- and 3s-electrons results in a reduction of the 3s-electron density at the nucleus, and, therefore, the electron density at the nucleus of Fe(II) is smaller than that of Fe(III). Because $|\Psi(0)|^2$ and the isomer shift are negatively correlated [25], the isomer shift of Fe(II) is larger than that of Fe(III). Hence, the reduction of the isomer shift for the surface octahedral iron ions should be interpreted as an electron redistribution in which they lose their electron charge, becoming more positive.

Table 1
Comparison of the Mössbauer parameters (IS – isomer shift, B_{hf} – hyperfine magnetic field) and the spectral component intensities for the clean and Au-decorated 4 ML (8 Å) $^{57}Fe_3O_4(0\,0\,1)$ surface layer on the 20 nm $^{56}Fe_3O_4(0\,0\,1)$ epitaxial film grown on MgO(0 0 1). The IS values refer to metallic iron. Numbers in parentheses are uncertainties of the last digit(s), resulting from the numerical fits using Voigt lines and a least square minimization procedure.

Spectral component	Hyperfine parameters	Clean surface	With 0.1 ML Au
A	IS (mm/s)	0.29 (1)	0.29 (1)
	B_{hf} (T)	47.9 (2)	47.8 (2)
	Intensity (%)	32.5 (20)	32.5 (20)
B	IS (mm/s)	0.66 (1)	0.66 (1)
	B_{hf} (T)	45.3 (2)	45.3 (2)
	Intensity (%)	34.9 (20)	33.0 (20)
S	IS (mm/s)	0.41 (2)	0.51 (3)
	B_{hf} (T)	42.8 (3)	41.8 (3)
	Intensity (%)	32.6 (30)	18.8 (30)
S_1	IS (mm/s)	–	0.58 (3)
	B_{hf} (T)	–	30.1 (3)
	Intensity (%)	–	11.8 (20)
S_2	IS (mm/s)	–	0.15 (2)
	Intensity (%)	–	3.7 (5)

Deposition of 0.1 ML Au caused visible changes in the CEMS spectrum, shown in Fig. 4b. The components (A) and (B) remained practically the same, regarding their parameters and intensities, but now, the remaining one third of the intensity, corresponding to the very surface, has been distributed among three components. The first one is similar to component (S) of the spectrum without gold, except for the isomer shift, which became more positive. Two new components are distinctly shown in Fig. 4b by shaded areas. The component S_1 should be associated with surface octahedral sites, at which gold adsorption contributed to a slight increase in the isomer shift and to a decrease in the hyperfine magnetic field B_{hf}. Such changes are indicative of a change (increase) in the d-electron densities at the surface octahedral Fe ions, which means a charge flow from the Au clusters to the oxide support. Nearly one-third of the surface Fe atoms are affected by such a charge transfer from the Au-clusters. More intriguing is the component S_2, with its small, positive isomer shift (unusual for oxides) and non-magnetic character. Such a value of IS can hardly be explained by the d-electron transfer only, and in our opinion must involve s-electrons. It is plausible that Fe ions at the support–cluster interface gain a metallic character with some 4s-electron density. The intensity of this component corresponds to 10% of the surface iron atoms, and this amount correlates well with the surface area covered by the gold clusters. Within a simple model that there is a direct transfer of s-electrons between Au and Fe, the s electron density corresponding to the observed IS value at the cluster–support interface is a half of that in metallic-Fe [25]. Hence, taking into account that the interface density of gold is twice that of iron, we can estimate the charge transfer of the s-electrons from gold to iron as about 0.25 electron per one gold atom.

The following picture of the electron charge redistribution induced by the Au clusters emerges from the Mössbauer data that are summarized in Table 1: a strong cluster–support interaction causes metallization of the Fe ions at the Au/magnetite interface, while the surface Fe ions outside the perimeter of the Au clusters are pushed to a lower valence state. Remarkably, this is a widespread effect, as indicated in the cartoon in Fig. 4. The gold adsorbate, covering an area less than 10% of the surface, influences the electronic structure of about 30% of the Fe surface atoms via electron transfer, resulting in positively charged gold clusters. Taking into account the surface density and diameter of the gold clusters at the 0.1 Au coverage (roughly 1 cluster per 10 nm^2 and 0.8 nm, respectively) one can estimate that the electron transfer touches Fe atoms at distances up to 1 nm from a gold cluster, under assumption that the effect has truly surface character.

4. Conclusions

We studied interaction between metallic nano-clusters and an oxide support. Gold deposition on epitaxially grown octahedral Fe_3O_4(0 0 1)/MgO(0 0 1) surface resulted in formation of two- and three-dimensional Au clusters. The STM analysis showed that the Au nucleation process is completed below a nominal coverage of 0.3 ML, and then, at larger coverages, the three-dimensional growth mode is dominant. A positive shift of the electron binding energy was observed in the Au 4f core excitations for the smallest clusters. The source of this relatively low (0.4 eV) BE shift can be assigned to three overlapping effects: the positive cluster charging due to both (1) the photo-ionization process (final state effect) and (2) the particle–support interaction, and (3) the surface effect resulting in a negative shift. This implies modification of the electronic structure, which is crucial for the catalytic properties. Based on the analysis of the Mössbauer spectra we showed that for the Au–Fe_3O_4(0 0 1) system this modification lies in the charge transfer between the cluster and the support resulting in the valence shift of surface Fe atoms toward a lower oxidation state. It is remarkable that for the conducting Fe_3O_4(0 0 1) surface the charge flow spreads over a surface area considerably exceeding the area occupied by the gold clusters. On the other hand, locally, at the cluster–support interface, the iron ions gain a metallic character by proximity of gold atoms. By simple arguments, such effects make the gold clusters positively charged, because electrons must be transferred from the clusters to the support. The electron transfer from Au to the support is limited by the ability of an iron ion to accept electrons and by the number of iron ions involved in this process, which must be neighbors to a gold cluster. With increasing cluster size, this number certainly grows more slowly than the number of the gold atoms per cluster. Hence, while the total positive charge of the clusters increases with increasing size, the charge per single gold atom decreases. This explains why only the smallest clusters become catalytically active [5].

Acknowledgments

This work was supported in part by the Polish Ministry of Science and Higher Education (in particular, grant No. 2633/H03/2007/32) and by the Team Program of the Foundation for Polish Science, co-financed by the EU European Regional Development Fund.

References

[1] M. Bäumer, H.-J. Freund, Progr. Surf. Sci. 61 (1999) 127.
[2] C.R. Henry, Progr. Surf. Sci. 80 (2005) 92.
[3] W.T. Wallace, B.K. Min, D.W. Goodman, Top. Catal. 34 (2005) 17.
[4] M. Haruta, Catal. Today 36 (1997) 153.
[5] K.T. Rim, D. Eom, L. Liu, E. Stolyarova, J.M. Raitano, S.W. Chan, M. Flytzani-Stephanopoulos, G.W. Flynn, J. Phys. Chem. C 113 (2009) 10198.
[6] N. Spiridis, B. Handke, T. Slezak, J. Barbasz, M. Zajac, J. Haber, J. Korecki, J. Phys. Chem. B 108 (2004) 14356.
[7] J. Korecki, B. Handke, N. Spiridis, T. Slezak, I. Flis-Kabulska, J. Haber, Thin Solid Films 412 (2002) 14.
[8] G. Tarrach, D. Burgler, T. Schaub, R. Wiesendanger, H.-J. Güntherodt, Surf. Sci. 285 (1993) 1.
[9] C. Seoighe, J. Naumann, I.V. Shvets, Surf. Sci. 440 (1999) 116.
[10] F.C. Voogt, Ph.D. Thesis, Departments of chemical physics and nuclear solid state physics, University of Groningen, Netherlands, 1998.
[11] A.V. Mijiritskii, D.O. Boerma, Surf. Sci. 486 (2001) 73.
[12] J.M. Gaines, P.J.H. Bloemen, J.T. Kohlhepp, C.W.T. Bulle-Lieuwma, R.M. Wolf, A. Reinders, R.M. Jungblut, P.A.A. van der Heijden, J.T.W.M. van Eemeren, J. aan de Stegge, W.J.M. de Jonge, Surf. Sci. 373 (1997) 85.
[13] S.A. Chambers, S.A. Joyce, Surf. Sci. 420 (1999) 111;
S.A. Chambers, S. Thevuthasan, S.A. Joyce, Surf. Sci. 450 (2000) L273.
[14] B. Stanka, W. Hebenstreit, U. Diebold, S.A. Chambers, Surf. Sci. 448 (2000) 49.
[15] A. Subagyo, K. Sueska, J. Phys.: Conf. Ser. 61 (2007) 1102.
[16] G. Mariotto, S. Murphy, I.V. Shvets, Phys. Rev. B 66 (2002) 245426.
[17] R. Pentcheva, F. Wendler, H.L. Meyerheim, W. Moritz, N. Jedrecy, M. Scheffler, Phys. Rev. Lett. 94 (2005) 126101.
[18] N. Spiridis, J. Barbasz, Z. Lodziana, J. Korecki Phys. Rev. B 74 (2006) 155423.
[19] K. Jordan, S. Murphy, I.V. Shvets, Surf. Sci. 600 (2006) 5150.
[20] G.K. Wertheim, S.B. DiCenzo, D.N.E. Buchanan, Phys. Rev. B 33 (1986) 5384.
[21] Y. Kitsudo, A. Iwamoto, H. Matsumoto, K. Mitsuhara, T. Nishimura, M. Takizawa, T. Akita, Y. Maeda, Y. Kido, Surf. Sci. 603 (2009) 2108.
[22] H.-G. Boyen, A. Ethirajan, G. Kästle, F. Weigl, P. Ziemann, Phys. Rev. Lett. 94 (2005) 016804.
[23] P.H. Citrin, G.K. Wertheim, Phys. Rev. Lett. 41 (1978) 1425.
[24] P. Torelli, L. Giordano, S. Benedetti, P. Luches, E. Annese, S. Valeri, G. Pacchioni, J. Phys. Chem. C 113 (2009) 19957.
[25] N.N. Greenwood, T.C. Gibb, Mössbauer Spectroscopy, Chapman and Hall, London, 1971.